Acoustic radiation force on cylindrical shells in a plane standing wave

2005 J. Phys. A: Math. Gen. 38 9395

(http://iopscience.iop.org/0305-4470/38/42/016)

INSTITUTE OF PHYSICS PUBLISHING JOURNAL OF PHYSICS A: MATHEMATICAL AND GENERAL

J. Phys. A: Math. Gen. **38** (2005) 9395–9404 doi:10.1088/0305-4470/38/42/016

Acoustic radiation force on cylindrical shells in a plane standing wave

F G Mitri

Mayo Clinic College of Medicine and Foundation, Department of Physiology and Biomedical Engineering, Ultrasound Research Laboratory, 200 First Street SW, Rochester, MN 55905, USA

E-mail: mitri@ieee.org and mitri.farid@mayo.edu

Received 19 July 2005, in final form 8 September 2005
Published 5 October 2005
Online at stacks.iop.org/JPhysA/38/9395

Abstract

In this paper, the radiation force per length resulting from a plane standing wave incident on an infinitely long cylindrical shell is computed. The cases of elastic and viscoelastic shells immersed in ideal (non-viscous) fluids are considered with particular emphasis on their thickness and the content of their interior hollow spaces. Numerical calculations of the radiation force function Y_{st} are performed. The fluid-loading effect on the radiation force function curves is analysed as well. The results show several features quite different when the interior hollow space is changed from air to water. Moreover, the theory developed here is more general since it includes the results on cylinders.

PACS number: 43.25.+y

1. Introduction

The procedure to position and manipulate materials using sound or ultrasound waves is called acoustic levitation [1, 2]. The free suspension of material samples is often necessary for certain types of physical property measurements. This technique has been successfully used in space applications for positioning materials (such as samples of small liquid and solid materials with diameters ranging from micrometres to millimetres) in the microgravity environment of a stationary ultrasonic field [3]. Moreover, acoustic levitation has been applied in different research areas, for example, in fluid dynamics [4, 5], materials science [6] and analytical chemistry [7].

The physical phenomenon behind the acoustic levitation is, indeed, the acoustic radiation force resulting from the standing wave field. Rayleigh [8] was the first to investigate the effect of the acoustic radiation force on objects. Later, King [9] studied the acoustic radiation force acting on a sphere in a standing-wave field. Furthermore, various aspects of the acoustic radiation force were investigated [10–19].

Nonetheless, the acoustic radiation force on cylindrically shaped structures has received significantly less attention. The first theoretical study dates back to the early work of Awatani [20] who computed the radiation force caused by progressive and stationary plane acoustic waves impinging on a rigid cylinder immersed in a compressible fluid. His calculations were performed within a very limited range of frequency ($0 \leqslant ka \leqslant 5$). Later, Hasegawa *et al* [21] extended his study and computed the radiation force due to progressive acoustic waves for different elastic cylinder materials. Wu *et al* [22] gave a long-wavelength approximation for the radiation force on a rigid cylinder for the situation where the cylinder's axis is constrained to be parallel to the equi-amplitude surfaces of a plane standing wave. Soon after, Hasegawa *et al* [23] developed a more general theory to study the acoustic radiation force on elastic, cylindrical and spherical shells placed in a progressive wave field.

Our purpose in the present study is to extend the work previously developed [24, 25] by analysing and developing analytical equations for the acoustic radiation force on *cylindrical shells* (with hollow) placed in a plane standing wave and immersed in ideal fluids. Although a theory has been recently developed for spherical shells in standing waves for drug delivery applications in the medical field [26], it is of particular interest to study the radiation force on tubular (elastic or viscoelastic) specimens in non-contact and non-destructive procedures for space-related applications. The theory gives *a priori* knowledge about the magnitude of the force used to levitate the specimens and manipulating them non-destructively. By performing acoustic levitation experiments in a low-gravity environment we can (for a time) reduce or remove the effects of gravity from the problem, all the while maintaining the advantages of non-contact manipulation that acoustics provides. In this work, the radiation force per length on elastic and viscoelastic cylindrical shells is expressed using a dimensionless factor called the acoustic radiation force function Y_{st}—which is the radiation force per unit energy density and unit cross-sectional surface—for a standing wave. Numerical calculations are performed for a few examples including brass elastic and polymer-type viscoelastic cylindrical shells filled with the same fluid or with a different fluid than their interior hollow spaces. Particular attention is directed to the thicknesses of the shells as well as the fluid surrounding their exterior. The fluid-loading effect on the Y_{st} curves is also analysed by considering a high-density fluid surrounding the shells.

2. Method

The acoustic radiation force is commonly interpreted as the time-averaged force, and calculated by averaging the radiation–stress tensor expressed in terms of the total scattering velocity potential or pressure in an ideal fluid. It is, therefore, essential to calculate first the total linear acoustic scattering field disturbed by the shell for the purpose of obtaining the radiation force.

2.1. Acoustic scattering by a cylindrical shell in a plane standing wave

Consider a solid cylindrical shell of outer radius a and inner radius b. Its axis is taken to coincide with the z-axis of the coordinate cylindrical system (r, θ, z). The outside and inside fluid mass density are ρ and ρ', respectively, and the shell's mass density is denoted by ρ^*. The cylindrical shell's centre is assumed to be placed at a distance h from the nearest pressure antinode of a plane stationary wave at normal incidence with respect to the z-axis (figure 1). The cylindrical shell is assumed to be immersed in an ideal compressible fluid so that the viscous and thermal effects can be neglected.

The incident velocity potential is expressed by

$$\Phi_{\mathrm{inc}}^{\mathrm{st}} = \Phi_0 \, \mathrm{e}^{-\mathrm{i}\omega t} \{ \mathrm{e}^{\mathrm{i}k(x+h)} + \mathrm{e}^{-\mathrm{i}k(x+h)} \}, \tag{1}$$

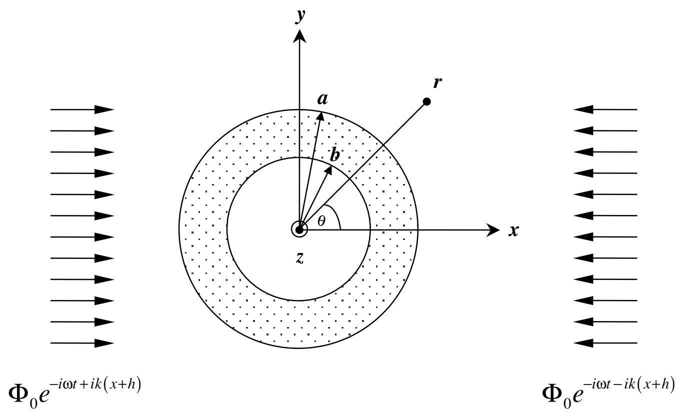

Figure 1. 2D-frontal view of a circular cylindrical shell placed in a plane standing wave acoustic field. The shell's axis is constrained to be parallel to the equi-amplitude surfaces of the plane acoustic standing wave.

where Φ_0 is the amplitude, $k = \omega/c$ is the wave number in the fluid medium and c is the sound velocity in the exterior fluid medium.

In a system of cylindrical coordinates, equation (1) can be rewritten as

$$\Phi_{\mathrm{inc}}^{\mathrm{st}} = \sum_{n=0}^{\infty} \Lambda_n \varepsilon_n i^n J_n(kr)\cos(n\theta)\,\mathrm{e}^{-\mathrm{i}\omega t}, \tag{2}$$

where $\Lambda_n = \Phi_0\{\mathrm{e}^{\mathrm{i}kh} + (-1)^n\,\mathrm{e}^{-\mathrm{i}kh}\}$, ε_n is the Neumann factor which is defined by $\varepsilon_0 = 1$, and $\varepsilon_j = 2$, $j = 1, \ldots, n$, and $J_n(\cdot)$ is the Bessel function of the first kind of order n.

The wave velocity in the core material of the shell is expressed by

$$\mathbf{v}_{\mathrm{int}} = -\nabla\Phi_{\mathrm{int}} + \nabla\times\Psi_{\mathrm{int}}, \tag{3}$$

where Φ_{int} and $\Psi_{\mathrm{int}}(0, 0, \Psi_{\mathrm{int}})$ are the scalar and vector potentials expressed in cylindrical coordinates by

$$\begin{aligned}\Phi_{\mathrm{int}} &= \sum_{n=0}^{\infty} \Lambda_{n,l}\varepsilon_n i^n[A_n J_n(k_{\mathrm{l}}r) + B_n Y_n(k_{\mathrm{l}}r)]\cos(n\theta)\,\mathrm{e}^{-\mathrm{i}\omega t},\\ \Psi_{\mathrm{int}} &= \sum_{n=0}^{\infty} \Lambda_{n,s}\varepsilon_n i^n[C_n J_n(k_{\mathrm{s}}r) + D_n Y_n(k_{\mathrm{s}}r)]\sin(n\theta)\,\mathrm{e}^{-\mathrm{i}\omega t},\end{aligned} \tag{4}$$

where

$$\Lambda_{n,l} = \Phi_0\{\mathrm{e}^{\mathrm{i}k_{\mathrm{l}}h} + (-1)^n\,\mathrm{e}^{-\mathrm{i}k_{\mathrm{l}}h}\}, \qquad \Lambda_{n,s} = \Phi_0\{\mathrm{e}^{\mathrm{i}k_{\mathrm{s}}h} + (-1)^n\,\mathrm{e}^{-\mathrm{i}k_{\mathrm{s}}h}\} \qquad \text{and} \qquad k_{\mathrm{l}} = \omega/c_{\mathrm{l}}$$

is the compressional wave number, c_{l} is the compressional wave velocity, $k_{\mathrm{s}} = \omega/c_{\mathrm{s}}$ is the shear wave number, c_{s} is the shear wave velocity, $Y_n(\cdot)$ is the cylindrical Bessel function of the second kind and A_n, B_n, C_n and D_n are unknown coefficients.

The wave velocity in the *ideal* fluid filled in the hollow region of the shell is expressed in cylindrical coordinates as

$$\Phi_{\mathrm{f}} = \mathrm{e}^{-\mathrm{i}\omega t}\sum_{n=0}^{\infty} \Lambda_{n,f}\varepsilon_n i^n E_n J_n(k_{\mathrm{f}}r)\cos(n\theta), \tag{5}$$

where $\Lambda_{n,f} = \Phi_0\{\mathrm{e}^{\mathrm{i}k_{\mathrm{f}}h} + (-1)^n\,\mathrm{e}^{-\mathrm{i}k_{\mathrm{f}}h}\}$, $k_{\mathrm{f}} = \omega/c_{\mathrm{f}}$, c_{f} is the compressional wave velocity in the interior fluid and E_n is an arbitrary coefficient.

The scattered velocity potential is expressed as

$$\Phi_{\mathrm{sc}}^{\mathrm{st}} = \sum_{n=0}^{\infty} \Lambda_n \varepsilon_n i^n S_n H_n^{(1)}(kr)\cos(n\theta)\,\mathrm{e}^{-\mathrm{i}\omega t}, \tag{6}$$

where $H_n^{(1)}(\cdot)$ is the Hankel function of the first kind of order n and S_n is the unknown coefficient to be determined from the following boundary conditions at $r = a$ and $r = b$ (a and b being the outer and inner radius of the cylindrical shell, respectively):

(1) the pressure in the fluid equals the normal component of stress in the solid at the interface,
(2) the normal (radial) component of displacement (or velocity, respectively) of the fluid must be equal to the normal component of displacement (or velocity, respectively) of the solid at the interface,
(3) the tangential components of shearing stress must vanish at the surface of the solid.

The general solution for S_n is given by

$$S_n = \left[\frac{-F_n J_n(x) + x J_n'(x)}{F_n H_n^{(1)}(x) - x H_n^{(1)'}(x)}\right], \tag{7}$$

where $x = ka$ and the coefficients F_n are explicitly given in [27].

The term S_n is a complex number that can be written as

$$S_n = (\alpha_n + \mathrm{i}\beta_n). \tag{8}$$

Thus, the total (incident + scattered) velocity potential is expressed by

$$\Phi_{\mathrm{t}}^{\mathrm{st}} = \sum_{n=0}^{\infty} \Lambda_n \varepsilon_n i^n (U_n + \mathrm{i}V_n)\cos(n\theta)\,\mathrm{e}^{-\mathrm{i}\omega t}, \tag{9}$$

where U_n and V_n are given by the following equations:

$$U_n = (1+\alpha_n)J_n(kr) - \beta_n Y_n(kr), \qquad V_n = \beta_n J_n(kr) + \alpha_n Y_n(kr). \tag{10}$$

2.2. Acoustic radiation force on a cylindrical shell placed in a plane standing wave

The total averaged force caused by acoustic waves on a boundary moving at a small velocity of the first order in an ideal fluid is given by [11]

$$\langle \mathbf{F}\rangle = -\iint_s \left[\left(\frac{1}{2}\frac{\rho}{c^2}\left\langle\left(\frac{\partial \Psi^{\mathrm{st}}}{\partial \mathrm{t}}\right)^2\right\rangle - \frac{1}{2}\rho\langle|\nabla\Psi^{\mathrm{st}}|^2\rangle\right)\mathbf{n} + \rho\langle(\upsilon_n\mathbf{n} + \upsilon_t\mathbf{t})\upsilon_n\rangle\right]\mathrm{d}S, \tag{11}$$

where S is the boundary at its *equilibrium* position and $\langle\cdot\rangle$ stands for time average,

$$\Psi^{\mathrm{st}} = \mathrm{Re}\left[\Phi_{\mathrm{t}}^{\mathrm{st}}\right] = \sum_{n=0}^{\infty} \varepsilon_n R_n \cos(n\theta), \tag{12}$$

in which the functions $R_n = \mathrm{Re}[(i)^n (U_n(kr) + \mathrm{i}V_n(kr))\Lambda_n\,\mathrm{e}^{-\mathrm{i}\omega t}]$ and $-\nabla\Psi^{\mathrm{st}}$ is the first-order particle velocity of the boundary and $\Phi_{\mathrm{t}}^{\mathrm{st}}$ is the total velocity potential in the fluid medium described in equation (9) and $\upsilon_n\mathbf{n}$ and $\upsilon_t\mathbf{t}$ are the normal and tangential components of the particle velocity of the boundary, respectively.

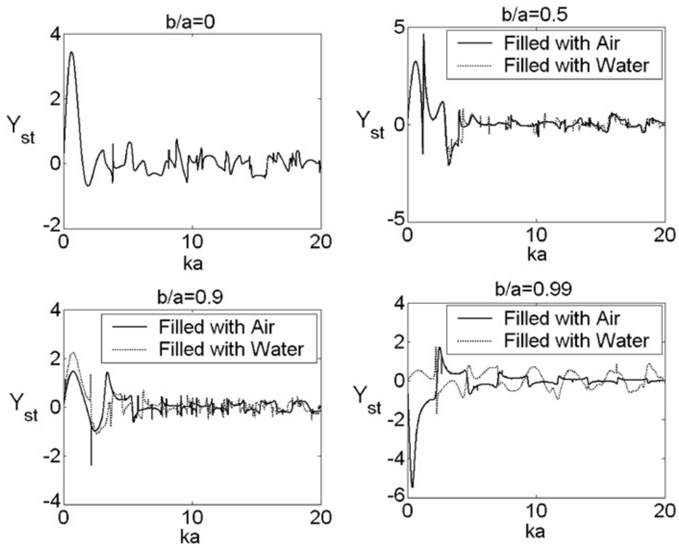

Figure 2. The radiation force function curves for brass elastic cylindrical shells placed in a standing wave and immersed in water. Their interior hollow regions are filled with air (solid line) or water (dotted line) for four thickness (b/a) values. One notices the great change between the air-filled and water-filled solutions.

In the direction of wave propagation (x-direction), the radiation force per unit length of the shell is expressed as [25]

$$\langle F_x \rangle_{st} = Y_{st} S_c \langle E_p \rangle \sin(2kh), \tag{13}$$

where $S_c = 2a$ is the cross-sectional area for a unit-length cylindrical shell and $\langle E_p \rangle = (1/2)\rho k^2 |\Phi_0|^2$ is the mean energy density of the incident *progressive* plane wave (where its velocity potential is given by $\Phi_{inc}^p = \Phi_0 \,e^{-i(\omega t - kx)}$). Y_{st} is the radiation force function that depends on the scattering and absorption properties of the target and the radiation force per unit cross section and unit energy density. The dimensionless factor Y_{st} is defined as the radiation force function for standing or stationary waves, and expressed by [25]

$$Y_{st} = \frac{4}{x} \sum_{n=0}^{\infty} (-1)^{n+1} [\beta_n (1 + 2\alpha_{n+1}) - \beta_{n+1}(1 + 2\alpha_n)] \tag{14}$$

where $x = ka$.

3. Numerical results and discussion

Equation (14) is used to compute the acoustic radiation force function Y_{st} for various materials. The results are shown in figures 2–8 with particular emphasis on the shells' thicknesses and the content of their interior hollow space regions.

The radiation force function Y_{st} curves are plotted as a function of the size parameter $x = ka$ (a being the outer radius of the cylindrical shell) within the range of frequency defined by $0 \leqslant x \leqslant 20$ in intervals of 0.001. It is very important to choose a sufficiently small sampling step since resonance peaks are very sharp and a wrong sampling may lead to false curves. It is also verified that the Y_{st} curves do not vary significantly when the step value is decreased. The mechanical parameters of various materials used in the calculations are listed in table 1.

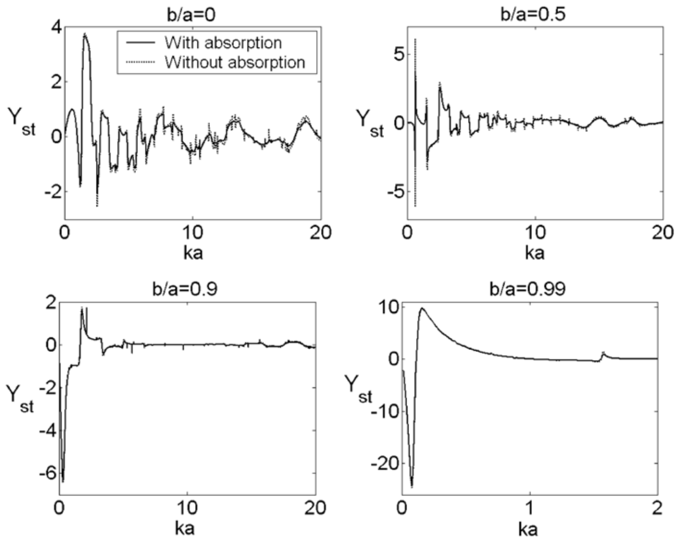

Figure 3. The radiation force function curves for lucite cylindrical shells placed in a standing wave and immersed in water. Their interior hollow regions are filled with air for four thickness (b/a) values with and without absorption.

Table 1. Material parameters used in the numerical calculations.

Material	Mass density (10^3 kg m^{-3})	Compressional velocity (m s^{-1})	Shear velocity (m s^{-1})	Normalized longitudinal absorption γ_1	Normalized shear absorption γ_2
Air	0.001 23	340	–	–	–
Brass	8.1	3830	2050	–	–
Lucite	1.191	2690	1340	0.0035	0.0053
Mercury	13.6	1407	–	–	–
Polyethylene	0.957	2430	950	0.0073	0.022
Water	1.00	1500	–	–	–

Figure 2 shows a comparison between the Y_{st} curves for brass elastic shells immersed in water and filled with air or water for four thickness values. The case where $b/a = 0$ corresponds to the radiation force function for a cylinder. One notices the great change between the air-filled and water-filled solutions, especially for thin shells $(b/a = 0.99)$. Nevertheless, the change is less prominent for thick shells. In addition, the brass material is heavier than the propagation medium, so the cylindrical shells are attracted to a pressure node ($Y_{st} > 0$) in the low *ka* range; however, for thin shells filled with air $(b/a = 0.99)$, $Y_{st} < 0$ and hence, the shells are attracted to a pressure antinode.

Figures 3 and 4 show the radiation force function curves for non-absorbent and absorbent lucite shells filled with air or water, respectively. Longitudinal and shear waves absorption in lucite (and polyethylene; next paragraph) is linearly dependent on frequency and is modelled by introducing complex wave numbers. It is important to notice the high resonance peak observed at low *ka* values for the case of thin shells filled with air (figure 3). In contrast, for the case of thin shells filled with water (figure 4), the high resonance peak does disappear. This behaviour is expected since the acoustic radiation force is proportional to the *gradient* of the energy density. Here, when air fills the shell's interior hollow space, it creates a high acoustic

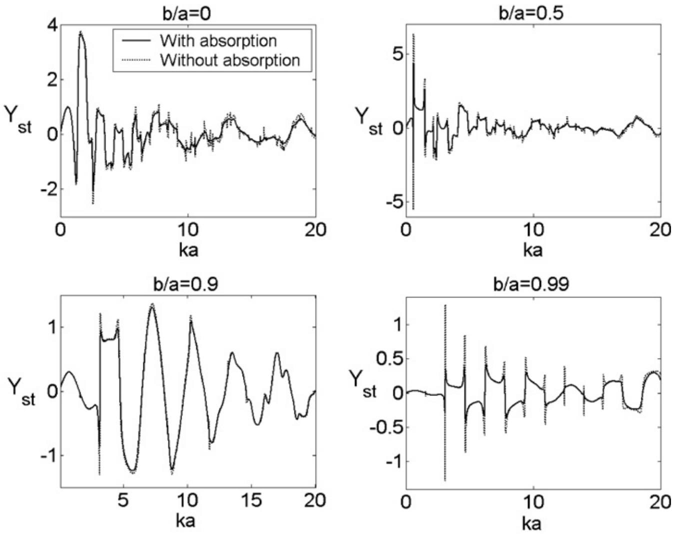

Figure 4. The same as in figure 3 except that the interior hollow regions are filled with water.

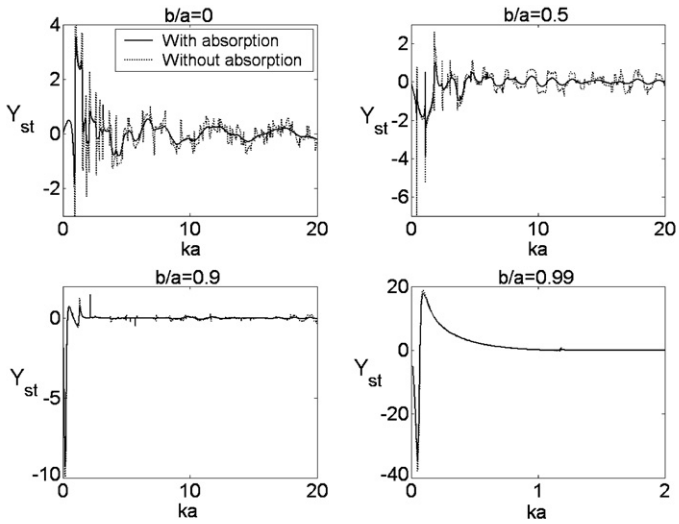

Figure 5. The comparison of the Y_{st} curves for non-absorbent and absorbent polyethylene cylindrical shells immersed in water and filled with air.

impedance gradient that *increases* when the shell's thickness *decreases*. Therefore, sound (or ultrasound) reflection is high. Consequently, the net radiation force per cross section acting on the cylindrical shell is greater than for the case where the interior hollow region is filled with water that facilitates sound (or ultrasound) transmission through the scattering area.

Figures 5 and 6 show the acoustic radiation force function for absorbent and non-absorbent polyethylene cylindrical shells filled with air or water, respectively. Notice that the damping of all peaks appears more clearly for this material whose normalized absorption coefficients are greater than lucite (table 1).

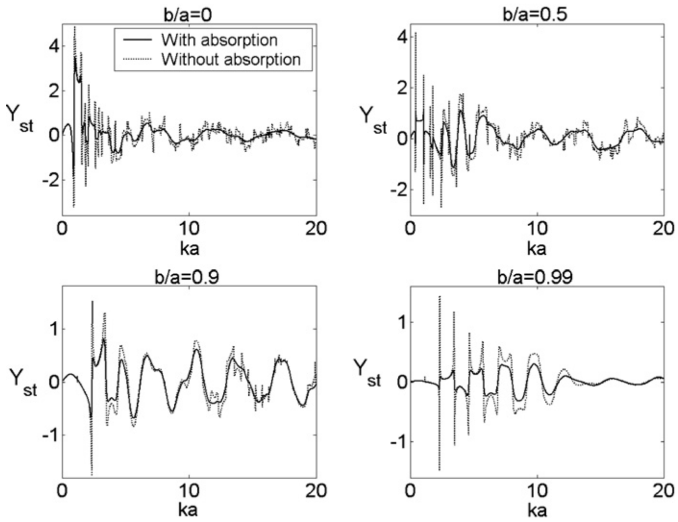

Figure 6. The same as in figure 5 but the shells' interior hollow regions are filled with water. Obviously, the damping of the resonance peaks appears more clearly for this material whose normalized absorption coefficients are greater than lucite.

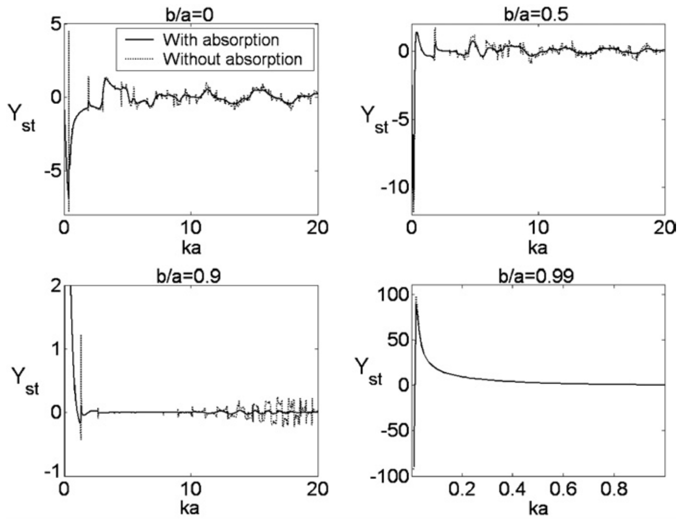

Figure 7. The Y_{st} curves for polyethylene cylindrical shells immersed in mercury and filled with air with and without absorption. The fluid-loading has a significant impact on the Y_{st} curves; a 'giant resonance' peak appears clearly at low *ka* values. Furthermore, the acoustic radiation force is not greatly affected by sound absorption inside the viscoelastic material when immersed in a high density fluid.

Figures 7 and 8 show additional calculations of the acoustic radiation force function Y_{st} for absorbent and non-absorbent cylindrical shells immersed in mercury and filled with air or water, respectively. Obviously, the fluid-loading effect on the radiation force function curves is very significant. The fluid-loading produces interactions between various resonance vibrational modes that can have a significant impact on the radiation force. This is clearly observed especially in figure 7 where a 'giant resonance peak' appears at low *ka*. A similar

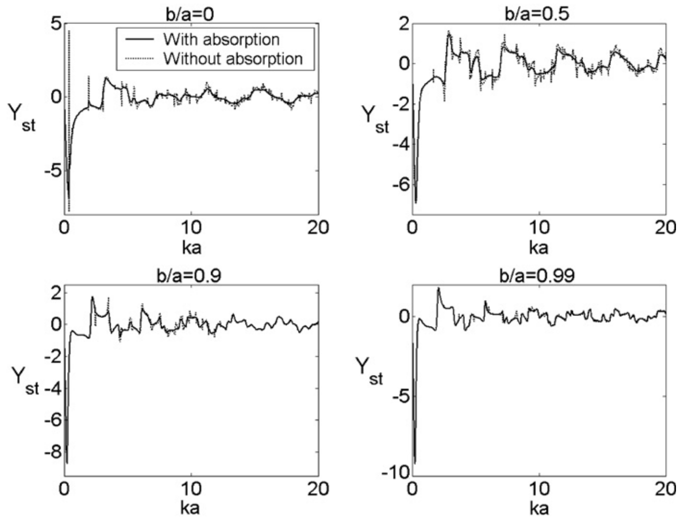

Figure 8. The same as in figure 7 but the shells' interior hollow regions are filled with water.

behaviour was observed in acoustic backscattering from viscoelastic cylinders immersed in a high density fluid [28]. In an original paper, Hay and Schaafsma [29] discussed the nature of these 'giant resonance peaks' in the attenuation of sound in suspensions of viscoelastic spheres (placed in a plane progressive wave) at low frequency. These resonances are properly identified as associated with subsonic Rayleigh waves [30]. Our analysis is the first to extend the results of the work done by Hay and Schaafsma on acoustic scattering for the case of the *acoustic radiation force* experienced by viscoelastic cylindrical shells placed in a *standing wave* field.

Furthermore, it is clearly shown from both figures 7 and 8 that the cylindrical shell, lighter than the propagation medium (mercury), is attracted to a pressure antinode ($Y_{\rm st} < 0$) in the low frequency region. Moreover, for high density fluids, the radiation force is not greatly affected by sound absorption inside the viscoelastic shells' materials.

4. Conclusion

In this work, an exact expression of the acoustic radiation force experienced by elastic and viscoelastic cylindrical shells immersed in *ideal* fluids and placed in a standing wave was developed. Analytical equations were derived for the time-averaged radiation force assuming the media outside and inside the shells are ideal compressible fluids. Numerical calculations of the radiation force function $Y_{\rm st}$ were performed for different materials. Particular emphasis was laid upon the absorption of sound by the viscoelastic material, and the loading effect of the surrounding fluid. The results indicated the ways in which the radiation force function curves were affected by variations in the shells' mechanical properties. Cylindrical shells were predicted to be attracted to pressure nodes when $Y_{\rm st} > 0$ and to pressure antinodes when $Y_{\rm st} < 0$, and the radiation force vanished for $kh = \pm(n\pi/2)$. If the cylindrical shell was centred on a pressure antinode, $n = 0$, and if it was centred on a pressure node $n = 1, 2, \ldots$. The magnitude of the radiation force was maximal when the shell was at the intermediate location defined by $kh = \pm(2n+1)\frac{\pi}{4}, n = 0, 1, \ldots$ These results have shown that the theory developed is more general since it has included the results on cylinders [25].

References

[1] Eller A 1968 *J. Acoust. Soc. Am.* **43** 170
[2] Brandt D T 2001 *Nature* **413** 474
[3] Collas P, Barmatz M and Shipley C 1989 *J. Acoust. Soc. Am.* **86** 777
[4] Tian Y, Holt R G and Apfel R E 1995 *Rev. Sci. Instrum.* **66** 3349
[5] Yarin A L, Pfaffenlehner M and Tropea C 1998 *J. Fluid Mech.* **356** 65
[6] Trinh E H 1985 *Rev. Sci. Instrum.* **56** 2059
[7] Bauerecker S and Neidhart B 1998 *J. Chem. Phys.* **109** 3709
[8] Rayleigh R W S 1902 *Phil. Mag.* **3** 338
[9] King L V 1934 *Proc. R. Soc.* A **147** 212
[10] Embleton T F W 1954 *J. Acoust. Soc. Am.* **26** 40
[11] Yosioka K and Kawasima Y 1955 *Acustica* **5** 167
[12] Maindanik G and Westervelt P J 1957 *J. Acoust. Soc. Am.* **29** 936
[13] Gor'kov L P 1962 *Sov. Phys. Dokl.* **6** 773
[14] Nyborg W L 1967 *J. Acoust. Soc. Am.* **42** 947
[15] Crum L A 1971 *J. Acoust. Soc. Am.* **50** 157
[16] Hasegawa T 1977 *J. Acoust. Soc. Am.* **61** 1445
[17] Asaki T J and Marston P L 1994 *J. Acoust. Soc. Am.* **96** 3096
[18] Doinikov A A 1996 *Phys. Rev.* E **54** 6297
[19] Mitri F G and Chen S 2005 *Phys. Rev.* E **71** 016306
[20] Awatani J 1955 *Mem. Inst. Sci. Ind. Osaka Univ.* **12** 95
[21] Hasegawa T, Saka K, Inoue N and Matsuzawa K 1988 *J. Acoust. Soc. Am.* **83** 1770
[22] Wu J, Du G, Work S S and Warshaw D M 1990 *J. Acoust. Soc. Am.* **87** 581
[23] Hasegawa T, Hino Y, Annou A, Noda H and Kato M 1993 *J. Acoust. Soc. Am.* **93** 154
[24] Haydock D 2005 *J. Phys. A: Math. Gen.* **38** 3279
[25] Mitri F G 2005 *Eur. Phys. J.* B **44** 71
[26] Mitri F G 2005 *Ultrasonics* **43** 681
[27] Mitri F G 2005 *Ultrasonics* **43** 271
[28] Mitri F G, Fellah Z E A and Chapelon J Y 2004 *J. Acoust. Soc. Am.* **115** 1411
[29] Hay A E and Schaafsma A S 1988 *J. Acoust. Soc. Am.* **85** 1124
[30] Hefner B T and Marston P L 2000 *J. Acoust. Soc. Am.* **107** 1930